Overtransmission of Rossby Waves at a Lower-Layer Critical Latitude in the Two-Layer Model

MATTHEW T. GLIATTO

Atmospheric and Oceanic Sciences Program, Princeton University, Princeton, New Jersey

ISAAC M. HELD

Geophysical Fluid Dynamics Laboratory, Princeton, New Jersey

(Manuscript received 5 March 2019, in final form 26 December 2019)

ABSTRACT

Rossby waves, propagating from the midlatitudes toward the tropics, are typically absorbed by critical latitudes (CLs) in the upper troposphere. However, these waves typically encounter CLs in the lower troposphere first. We study a two-layer linear scattering problem to examine the effects of lower CLs on these waves. We begin with a review of the simpler barotropic case to orient the reader. We then progress to the baroclinic case using a two-layer quasigeostrophic model in which there is vertical shear in the mean flow on which the waves propagate, and in which the incident wave is assumed to be an external-mode Rossby wave. We use linearized equations and add small damping to remove the critical-latitude singularities. We consider cases in which either there is only one CL, in the lower layer, or there are CLs in both layers, with the lower-layer CL encountered first. If there is only a CL in the lower layer, the wave's response depends on the sign of the mean potential vorticity gradient at this lower-layer CL: if the PV gradient is positive, then the CL partially absorbs the wave, as in the barotropic case, while for a negative PV gradient, the CL is a wave emitter, and can potentially produce overreflection and/or overtransmission. Our numerical results indicate that overtransmission is by far the dominant response in these cases. When an upper-layer absorbing CL is encountered, following the lower-layer encounter, one can still see the signature of overtransmission at the lower-layer CL.

1. Introduction

Rossby waves propagating on a zonal flow provide a useful theoretical simplification for the study of the fate of waves produced in midlatitudes and propagating into the tropics (Karoly and Hoskins 1982). Both the observed transient and stationary eddy momentum fluxes are poleward on average in the subtropics, a signature of equatorward propagation, but fall to zero near the equator, implying that these waves are predominately absorbed in the tropics. This absorption is understood as resulting from wave breaking that occurs because of the presence of a critical latitude (CL) in the upper troposphere where the zonal mean flow equals the phase speed of the wave. The work of Webster and Holton (1982), who examine the propagation of waves into the equatorial central Pacific where upper-level mean zonal winds are often westerly, provides observational support for the importance of the presence or absence of an upper-tropospheric CL. The phase speed spectra of the transient eddy momentum fluxes described in Randel and Held (1991) also support the importance of the upper-tropospheric CLs.

Yet, as illustrated by the schematic in Fig. 1, waves with a CL in the upper troposphere in the tropics will almost invariably first encounter a CL in the lower troposphere in the subtropics, because mean winds become more westerly with height in the troposphere. One is led to ask what factors control the wave–mean flow interaction at the lower-tropospheric CL. A line of argument that these should be minor might start with the fact that these waves have larger amplitudes in the upper troposphere than in the lower troposphere as measured by streamfunction amplitude or kinetic energy so that, in particular, the eddy momentum fluxes are primarily confined to the upper troposphere. But meridional particle displacement associated with a linear wave with streamfunction ψ and phase speed c is proportional to

Corresponding author: Matthew T. Gliatto, mgliatto07@gmail.com

DOI: 10.1175/JAS-D-19-0055.1

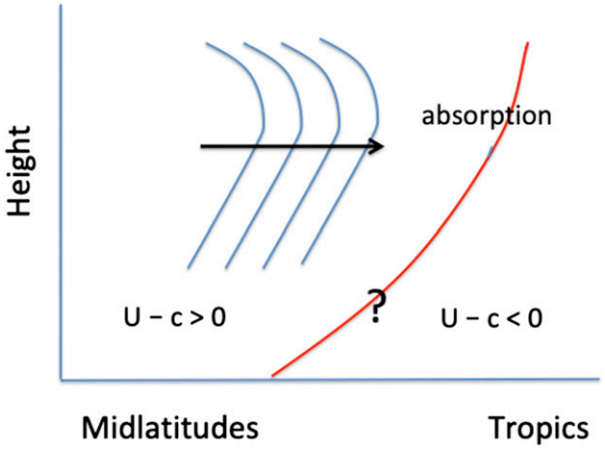

FIG. 1. Schematic showing a Rossby wave of a given phase speed c propagating from the midlatitudes toward the tropics. Note that the critical latitude moves equatorward as height increases, because the mean flow U becomes more westerly with height. The waves are absorbed by critical latitudes in the upper troposphere. This paper examines how they respond to those in the lower troposphere, which they encounter first.

$\psi/(U - c)$, where U is the mean zonal flow, so these meridional displacements can be relatively large in the lower troposphere, which suggests the potential for lower-tropospheric wave breaking and mean-flow modification.

Upper-level CL dynamics in the tropics are typically addressed with barotropic models, motivated in large part by weak coupling in the vertical in the tropics (Charney 1963). But this decoupling is not likely to be fully operative in the subtropics. The simplest model to begin addressing issues related to the lower-tropospheric CLs may be the two-layer quasigeostrophic model, keeping in mind that this model may overestimate vertical coupling in that it does not account for the increase in the radius of deformation with decreasing latitude. In this paper, we pose a scattering problem in the two-layer model, in which we shine a steady external Rossby wave on a shear zone that produces various configurations of CLs in the upper and lower layers. We study only the linear dissipative problem, in which weak damping removes the singularity at the steady linear CL. The incident wave is given the external-mode structure because of its prominence in the observed stationary wave field and qualitative similarity to transient eddies as well. In addition, it is horizontally propagating for parameters of interest, whereas the internal mode of the two-layer model is often horizontally evanescent in the same mean flow.

The classic barotropic Rossby wave CL has been studied in both linear and nonlinear settings. In most cases, the steady linear dissipative CL is at least partially absorbing, with absorption effectively complete if the flow is smooth enough (Dickinson 1968; Geisler and Dickinson 1974), but some reflection is possible even in this linear theory. In fact, significant reflection is possible even if there is no CL and no classical turning points (Potter et al. 2013). And the result that the dissipative CL is absorbing is dependent on the sign of the potential vorticity (PV) gradient at the CL—the absolute vorticity gradient in this barotropic case. If the PV gradient at the CL is negative, the CL becomes an emitter rather than an absorber. In the simplest one-layer case with one CL, propagation is possible on only one side of the CL, the side from which the wave is incident, so transmission is not possible and the emission of wave activity results in overreflection (Lindzen et al. 1980). Whether absorbing or emitting in the linear approximation, the fully nonlinear solution generally results in the PV gradient being mixed away, resulting in perfect reflection. The relevance of the linear or nonlinear picture depends on the efficiency of other processes that act to restore a significant gradient in the face of this mixing (Killworth and McIntyre 1985). We do not discuss the nonlinear problem here.

In the two-layer model, we also expect the sign of the PV gradient to be an important parameter in controlling the character of the lower-layer CL dynamics. But in this case, we are interested in mean flows in which the change in sign of the PV gradient in the lower layer is due to the vertical shear rather than horizontal curvature as in the barotropic case. If the PV gradient is reversed at the latitude of the lower-layer CL, the CL should become a wave emitter, as implied by the two-layer analog of the conservation law from which barotropic overreflection can be explained. However, in the two-layer case, there is potential for wave propagation on both sides of the CL, introducing the possibility of overtransmission along with, or instead of, overreflection. If the curvature is negligible, the sign of the PV gradient in the lower layer is determined by whether the shear is subcritical or supercritical, according to the Phillips (1956) criterion, and as a shorthand we refer to cases with negative and positive lower-layer PV gradients as supercritical and subcritical, respectively. The PV gradient is always positive in the upper layer in all of the two-layer cases examined here.

Lutsko et al. (2017) have recently described the structure of lower-layer momentum fluxes in the statistically steady state of a two-layer QG model. A role for the lower-layer critical latitude is evident in the space–time cospectra. They also find qualitatively similar momentum flux cospectra in an idealized dry GCM and in a Southern Hemisphere reanalysis, suggesting that

the two-layer model results have some relevance to the atmosphere.

The equations that we solve and the solution procedure are described for the barotropic special case in section 2 in some detail, to help orient readers unfamiliar with this Rossby wave scattering framework. The two-layer equations are described in section 3, followed by the results from these two-layer computations in section 4. Of particular interest is to determine whether or not overtransmission occurs in this idealized scattering setting. To our knowledge, this possibility has not been discussed in the literature on Rossby wave propagation. It does indeed occur, and in the concluding section we briefly discuss whether overtransmission has relevance to the patterns seen in Lutsko et al. and if it has any observable consequences for the atmosphere.

2. The barotropic case

We describe the previously studied barotropic case in some detail as an introduction to the Rossby wave scattering problem. As in Potter et al. (2013) and Halevy and Peltier (1985), we begin with the nondivergent barotropic vorticity equation on a β plane, linearized about a mean wind profile $U(y)$:

$$\frac{\partial \nabla^2 \psi'}{\partial t} + U(y)\frac{\partial \nabla^2 \psi'}{\partial x} + \left(\beta - \frac{\partial^2 U}{\partial y^2}\right)\frac{\partial \psi'}{\partial x} = 0, \tag{1}$$

where ψ' is the (perturbation) streamfunction. We consider steady-state solutions of the following form:

$$\psi' = \mathrm{Re}\{\psi(y)\exp[ik(x-ct)]\}. \tag{2}$$

Plugging this into Eq. (1) yields

$$\frac{\partial^2 \psi}{\partial y^2} + V(y)\psi(y) = 0, \tag{3}$$

where

$$V(y) = \frac{\beta - \partial^2 U/\partial y^2}{U(y) - c} - k^2. \tag{4}$$

To illustrate this barotropic problem, we work with a tanh mean wind profile:

$$U(y) = \frac{1}{2}u^*[\tanh(\alpha y) + 1], \tag{5}$$

where $U(y)$, and therefore also $V(y)$, approach constant values at both asymptotic limits in y. At the southern limit, Eq. (3) becomes

$$\frac{\partial^2 \psi}{\partial y^2} + V^-\psi(y) = 0$$

(V^- being the value of V at the southern limit), to which the general solution is

$$\psi(y) = A\exp(i\ell^- y) + B\exp(-i\ell^- y). \tag{6}$$

Likewise, the general solution at the northern limit is

$$\psi(y) = C\exp(i\ell^+ y) + D\exp(-i\ell^+ y). \tag{7}$$

Here $\ell(y) = \sqrt{V(y)}$ is the local meridional wavenumber, ℓ^- and ℓ^+ are its limits at negative and positive infinity, respectively, and A, B, C, and D are complex numbers. Note that if $V(y)$ is negative, then $\ell(y)$ will be imaginary, signifying that the wave is decaying.

We choose to imagine the wave source as being in the south (although we could have just as well chosen a wave incident from the north). That is, we imagine the problem as taking place in the Southern Hemisphere, with the Rossby wave originating in the Southern Hemisphere midlatitudes and propagating toward the tropics. This implies that D is zero. Furthermore, we are interested only in the ratio of B to A and the ratio of C to A. B/A is the reflection coefficient, which we denote as R, and C/A is the transmission coefficient, which we denote as T. So we have

$$\psi^-(y) = \exp(i\ell^- y) + R\exp(-i\ell^- y), \tag{8}$$

$$\psi^+(y) = T\exp(i\ell^+ y), \tag{9}$$

where $\psi^-(y)$ and $\psi^+(y)$ are the functions of y to which the solution converges at the southern and northern limits, respectively.

We now have enough information to solve for $\psi(y)$ numerically. We discretize the domain into n discrete values of y, each an equal distance Δy apart, evaluating $\partial^2\psi/\partial y^2$ with standard finite differencing. This gives us $n - 2$ equations for n variables. We can differentiate Eq. (8) to get

$$\frac{\partial \psi^-}{\partial y} + i\ell^-\psi^- = 2i\ell^-\exp(i\ell^- y) \tag{10}$$

and differentiate Eq. (9) to get

$$\frac{\partial \psi^+}{\partial y} = i\ell^+\psi^+, \tag{11}$$

thus eliminating R and T for the time being. We then discretize these boundary conditions to provide the two additional equations needed. Thus, we have n linear equations for n variables, and we invert the matrix for ψ at each value of y.

Following Potter et al. (2013), for the barotropic case, we nondimensionalize with a length scale of $1/k$ and a time scale of k/β. This gives us

$$V(y) = \frac{1 - \partial^2 U/\partial y^2}{U(y) - c} - 1 \tag{12}$$

leaving c as the only parameter in addition to the parameters describing $U(y)$: u^* and α. Given Galilean invariance, we could equivalently restrict c to vanish, adding a constant offset to $U(y)$, without altering the solutions.

If there is a CL, where $U = c$, this introduces a singularity to $V(y)$. To avoid this singularity, we consider a steady dissipative critical layer by adding a small amount of damping of the form $\varepsilon(y)\nabla^2\psi'$ to Eq. (1). We choose $\varepsilon(y)$ to have maximum amplitude ε_0 at the CL and to decrease to zero a distance of 2.5 nondimensional units away from the CL. This choice avoids the presence of damping near the boundaries, which creates spatial growth which in turn adversely affects the robustness of our numerical solution. The inclusion of the damping term makes $V(y)$ complex valued: it now becomes

$$V(y) = \frac{1 - \partial^2 U/\partial y^2}{U(y) - c - i\varepsilon(y)} - 1 \tag{13}$$

and so, as is well known, the singularity is avoided.

The momentum flux is given by

$$\overline{u'v'}(y) = -\frac{1}{2}\mathrm{Im}\left[\frac{\partial\psi}{\partial y}\psi^*(y)\right] \tag{14}$$

while the vorticity flux $\overline{v'\zeta'}$ is the convergence of the momentum flux:

$$\overline{v'\zeta'}(y) = -\frac{\partial}{\partial y}(\overline{u'v'}). \tag{15}$$

The linear steady-state enstrophy balance in the presence of damping expresses the balance between production due to downgradient vorticity flux and dissipation of enstrophy:

$$0 = -\gamma\overline{v'\zeta'} - \varepsilon\overline{\zeta'^2}, \tag{16}$$

where γ is the mean vorticity gradient. Away from the critical line, the perturbation vorticity remains finite in the limit $\varepsilon \to 0$, implying that the vorticity flux vanishes and the momentum flux is constant in latitude. Near the critical line, for small ε, the dissipation and the vorticity flux are both large in a region of width proportional to ε, the amplitude increasing and the width of this region decreasing with decreasing ε in such a way that the flux approaches a delta function (Dickinson 1969; Lindzen and Tung 1978; Held 1983). The sign of the delta function in the vorticity flux, and of the corresponding jump in the momentum flux, is determined by the requirement in the enstrophy budget that the vorticity flux be downgradient. If $\gamma(y_c) > 0$, then the momentum flux will increase as a function of y at the CL, while if $\gamma(y_c) < 0$, then the momentum flux will decrease at the CL. For the tanh profile considered, the wave is evanescent after the CL, so no transmission to large y is possible.

We define $\mathscr{R}$ to be the reflected momentum flux, normalizing by the momentum flux in the incident wave: $\mathscr{R} = |R|^2$. We expect partial absorption, $\mathscr{R} < 1$, in the subcritical case, while in the supercritical case, overreflection, $\mathscr{R} > 1$ is expected, as discussed by Lindzen and Tung (1978). We likewise define $\mathscr{T}$ to be the transmitted momentum flux, normalized by the momentum flux in the incident wave. But for the tanh profile, $\mathscr{T}$ will always be zero.

Except in the immediate vicinity of the CL, the solution, including the value of $\mathscr{R}$, should be insensitive to the value of ε_0 for small-enough ε_0. This insensitivity can be checked by repeating the calculation with different values of ε_0, taking care to use a sufficiently small Δy to resolve the rapid variations near the CL. We have verified that our model is sufficiently insensitive to the value of ε_0.

We begin by examining a specific mean wind profile [see Eq. (5)] and phase speed for the barotropic case, as shown in Fig. 2. With the phase speed c of 0.8 chosen for this figure, there is a negative PV gradient at the CL as the associated profile of $1 - \partial^2 U/\partial y^2$ shows. Overreflection is obtained, with $\mathscr{R} = 1.20$. Next, for this profile, we vary the phase speed and plot the momentum flux at the southern limit, normalized by the incident flux, as a function of the phase speed. This is shown in Fig. 3. This profile has a negative PV gradient at the CL within the range of phase speeds indicated by the two vertical red dashed lines, and positive PV gradient for all other c.

We see that for positive PV gradient at the CL, the reflection can be significant even though the CL must be partially absorbing. In the flow examined here, the reflection rises smoothly from near zero to values comparable to 1 as the phase speed approaches the region of reversed PV gradient. For these flows, the reflection is high because the wave encounters rapid variations in $V(y)$ before it reaches the CL. And for nearly all of the range between the two dashed red lines, where the PV gradient is reversed, the momentum flux at the southern boundary is positive, indicating overreflection.

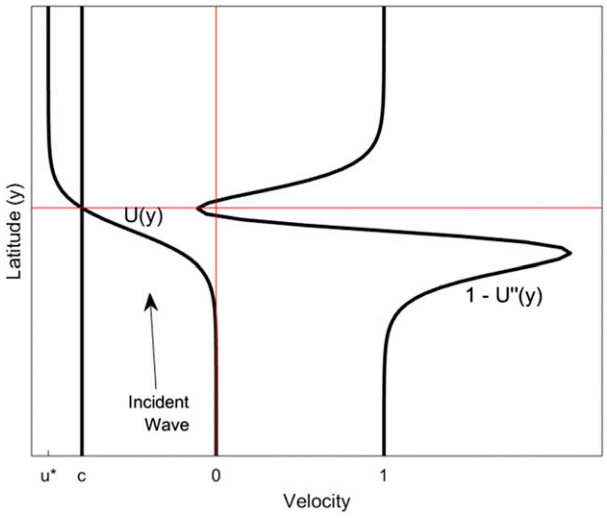

FIG. 2. Profiles of $U(y)$, c, and $\gamma(y) = 1 - \partial^2 U/\partial y^2$ for a barotropic case, with $u^* = -1$, $\alpha = 1.7$, and $c = -0.8$, so that $\gamma(y_c) = -0.110$. Also, $\mathscr{R} = 1.20$ and $\mathscr{T} = 0$.

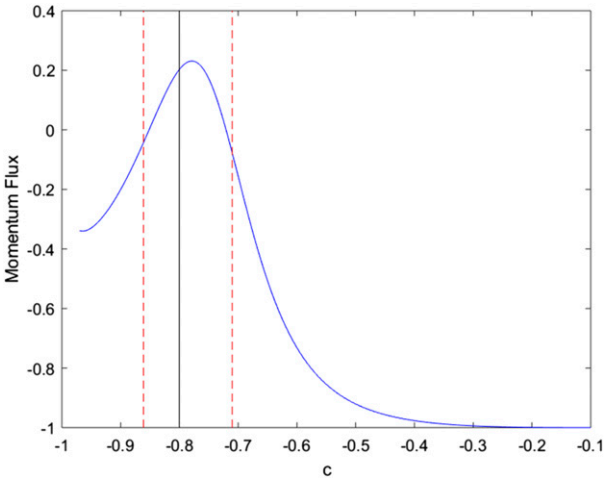

FIG. 3. Momentum flux at the southern limit as a function of phase speed c for the mean wind profile shown in Fig. 1. The value of $\gamma(y_c)$ is negative for phase speeds between the two vertical red dashed lines and is positive for all other c. The phase speed shown in Fig. 1 is indicated here by the solid black vertical line. Also, $\varepsilon = 0.007$ at the CL and $\Delta y = 0.0075$.

As an aside, it should be noted that if we were to examine the sech^2 profile (under which there would be two CLs) rather than the tanh profile, then the wave could propagate through both CLs into another propagating region, which means that $\mathscr{T}$ would be nonzero. This is consistent with the findings of Yamada and Okamura (1984) that there is overtransmission for this flow, $\mathscr{T} > 1$, if the PV gradient is negative at both CLs, a result that we have confirmed.

3. The baroclinic model

To address the question of the role of lower-tropospheric CLs, we use the equations of the two-layer quasigeostrophic (QG) Phillips model, examining Rossby wave propagation in the presence of vertical shear in the mean flow. Once again, we need to solve for the streamfunction, which the Phillips model prescribes as follows:

$$\frac{\partial q_j'}{\partial t} + U_j \frac{\partial q_j'}{\partial x} + Q_{jy} \frac{\partial \psi_j'}{\partial x} = 0, \quad (j = 1, 2), \tag{17}$$

where Q_{jy} and q_j', the gradient of the zonally averaged potential vorticity and the perturbation potential vorticity, are given by

$$\begin{aligned} q_j' &= \nabla^2 \psi_j' + (-1)^j (\psi_1' - \psi_2')/(2\lambda^2), \\ Q_{jy} &= \beta - \partial^2 U_j/\partial y^2 - (-1)^j (U_1 - U_2)/(2\lambda^2), \end{aligned} \tag{18}$$

where λ is the constant Rossby radius of deformation, and $U_1(y)$ and $U_2(y)$ are the mean wind profiles in the upper and lower layers, respectively. We nondimensionalize with the length scale of λ and a velocity scale of $\beta\lambda^2$, which means β and λ can be replaced with 1 in the above equations. We consider a steady-state solution of the following form:

$$\psi_j' = \mathrm{Re}\{\psi_j(y) \exp[ik(x - ct)]\}, \quad (j = 1, 2) \tag{19}$$

yielding a pair of differential equations:

$$\begin{aligned} \frac{\partial^2 \psi_1}{\partial y^2} + V_1(y)\psi_1(y) + \frac{1}{2}\psi_2(y) &= 0, \\ \frac{\partial^2 \psi_2}{\partial y^2} + V_2(y)\psi_2(y) + \frac{1}{2}\psi_1(y) &= 0, \end{aligned} \tag{20}$$

where

$$\begin{aligned} V_1(y) &= \frac{1 + c/2 - \partial^2 U_1/\partial y^2 - U_2(y)/2}{U_1(y) - c} - k^2, \\ V_2(y) &= \frac{1 + c/2 - \partial^2 U_2/\partial y^2 - U_1(y)/2}{U_2(y) - c} - k^2. \end{aligned} \tag{21}$$

The flow we consider is obtained by keeping our previous wind profile in the lower layer and simply adding a vertical shear $2S(y)$ to it in the upper layer:

$$\begin{aligned} U_1(y) &= \frac{1}{2} u^* [\tanh(\alpha y) + 1] + 2S(y), \\ U_2(y) &= \frac{1}{2} u^* [\tanh(\alpha y) + 1]. \end{aligned} \tag{22}$$

Initially, we will take S to be constant. The parameters are u^*, α, S, c, k, and ε_0.

Once again, the flow is asymptotically constant for large positive and negative values of y, and the solution in those regions is the sum of two waves, the external and the internal mode. These two modes are distinguished by their meridional wavenumbers, which are the square roots of the two eigenvalues of the matrix:

$$\begin{bmatrix} V_1(y) & \frac{1}{2} \\ \frac{1}{2} & V_2(y) \end{bmatrix}.$$

These meridional wavenumbers are given by

$$\ell_{\text{ex}}^2(y) = \frac{1}{2}\left\{ V_1(y) + V_2(y) + \sqrt{[V_1(y) - V_2(y)]^2 + 1} \right\},$$
$$\ell_{\text{in}}^2(y) = \frac{1}{2}\left\{ V_1(y) + V_2(y) - \sqrt{[V_1(y) - V_2(y)]^2 + 1} \right\}. \tag{23}$$

As before, the meridional wavenumbers are not always real. For most latitudes in most situations, $\ell_{\text{in}}(y)$ will be imaginary, signifying that the internal mode is evanescent, and for some latitudes in some situations, $\ell_{\text{ex}}(y)$ will also be imaginary, meaning the external mode is also decaying, rather than propagating. [Note that $\ell_{\text{ex}}^2(y) > \ell_{\text{in}}^2(y)$ for all y, so if the external mode is decaying, the internal mode must be as well.]

We are now in a position to solve for the boundary conditions. For $V_1(y)$, $V_2(y)$, $\ell_{\text{ex}}(y)$, and $\ell_{\text{in}}(y)$, we denote the northern limit with a superscript plus sign and the southern limit with a superscript minus sign. At the southern limit, Eq. (20) becomes

$$\psi_1''(y) + V_1^- \psi_1(y) + \frac{1}{2}\psi_2(y) = 0,$$
$$\psi_2''(y) + V_2^- \psi_2(y) + \frac{1}{2}\psi_1(y) = 0,$$

to which the general solution is

$$\psi_1(y) = A_1 \exp(i\ell_{\text{ex}}^- y) + B_1 \exp(-i\ell_{\text{ex}}^- y) + C_1 \exp(i\ell_{\text{in}}^- y) + D_1 \exp(-i\ell_{\text{in}}^- y),$$
$$\psi_2(y) = A_2 \exp(i\ell_{\text{ex}}^- y) + B_2 \exp(-i\ell_{\text{ex}}^- y) + C_2 \exp(i\ell_{\text{in}}^- y) + D_2 \exp(-i\ell_{\text{in}}^- y), \tag{24}$$

in which the coefficients satisfy the ratios $A_2/A_1 = B_2/B_1 = 2[(\ell_{\text{ex}}^-)^2 - V_1^-]$ and $C_2/C_1 = D_2/D_1 = 2[(\ell_{\text{in}}^-)^2 - V_1^-]$.

Likewise, at the northern limit, the general solution is

$$\psi_1(y) = E_1 \exp(i\ell_{\text{ex}}^+ y) + F_1 \exp(-i\ell_{\text{ex}}^+ y) + G_1 \exp(i\ell_{\text{in}}^+ y) + H_1 \exp(-i\ell_{\text{in}}^+ y),$$
$$\psi_2(y) = E_2 \exp(i\ell_{\text{ex}}^+ y) + F_2 \exp(-i\ell_{\text{ex}}^+ y) + G_2 \exp(i\ell_{\text{in}}^+ y) + H_2 \exp(-i\ell_{\text{in}}^+ y), \tag{25}$$

in which the coefficients satisfy the ratios $E_2/E_1 = F_2/F_1 = 2[(\ell_{\text{ex}}^+)^2 - V_1^+]$ and $G_2/G_1 = H_2/H_1 = 2[(\ell_{\text{in}}^+)^2 - V_1^+]$

As in the barotropic case, we need to specify the particular scattering problem being posed. We assume again that the wave is only incident from the south; this makes the F values and the H values equal to zero. We also assume that the incident wave consists of only the external mode, which makes the C values equal to zero. Finally, as with the barotropic case, we are interested only in the ratios of the coefficients to A_1, so we divide Eqs. (24) and (25) by A_1 to get

$$\psi_1^-(y) = \exp(i\ell_{\text{ex}}^- y) + R_{\text{ex1}} \exp(-i\ell_{\text{ex}}^- y) + R_{\text{in1}} \exp(-i\ell_{\text{in}}^- y),$$
$$\psi_2^-(y) = A_2 \exp(i\ell_{\text{ex}}^- y) + R_{\text{ex2}} \exp(-i\ell_{\text{ex}}^- y) + R_{\text{in2}} \exp(-i\ell_{\text{in}}^- y) \tag{26}$$

and

$$\psi_1^+(y) = T_{\text{ex1}} \exp(i\ell_{\text{ex}}^+ y) + T_{\text{in1}} \exp(i\ell_{\text{in}}^+ y),$$
$$\psi_2^+(y) = T_{\text{ex2}} \exp(i\ell_{\text{ex}}^+ y) + T_{\text{in2}} \exp(i\ell_{\text{in}}^+ y). \tag{27}$$

As in the one-layer case, we discretize the domain into n evenly spaced values of y and use the boundary conditions to complete the specification of the matrix to be inverted to solve for $\psi_1(y)$ and $\psi_2(y)$.

We also include damping with time scale ε_0 of potential vorticity to remove the singularity at any CLs. As before, we take $\varepsilon(y)$ to be a function of latitude that has local maxima of ε_0 at the CLs and that is 0 when y is more than 2.5 nondimensional units away from any CLs. We use $\varepsilon_0 = 0.001$.

In the baroclinic case, Eq. (14) is still true in each layer. To obtain the analog of Eq. (15) one needs to sum over the two layers, that is,

$$-\frac{\partial}{\partial y}\left(\sum_{j=1}^{2} \overline{u_j' v_j'} \right) = \sum_{j=1}^{2} \overline{v_j' q_j'}, \quad (j = 1, 2). \tag{28}$$

The eddy heat flux, which can be defined in each layer, is

$$H_j(y) = \overline{v_j'(\psi_1' - \psi_2')}, \quad (j = 1, 2). \tag{29}$$

For this two-layer model, $H_1(y) = H_2(y)$, and so we can refer to just one heat flux $H(y)$. As is well known, the heat, momentum, and PV fluxes are related by

$$-\frac{\partial}{\partial y}(\overline{u_1'v_1'}) - \frac{1}{2}H(y) = \overline{v_1'q_1'}(y),$$

$$-\frac{\partial}{\partial y}(\overline{u_2'v_2'}) + \frac{1}{2}H(y) = \overline{v_2'q_2'}(y). \tag{30}$$

The linear steady-state potential enstrophy balance plays the same role here as does the enstrophy balance in the barotropic case. In layer j we have

$$0 = -\gamma_j\overline{v_j'q_j'} - \varepsilon\overline{q_j'^2}, \tag{31}$$

where γ_j is the mean potential vorticity gradient in layer j:

$$\gamma_1(y) = 1 - \frac{\partial^2 U_1}{\partial y^2} + S(y),$$

$$\gamma_2(y) = 1 - \frac{\partial^2 U_2}{\partial y^2} - S(y).$$

If neither layer has a CL, then the total PV flux ("total" implies the sum over the two layers), or, equivalently the total momentum flux convergence, is uniformly 0. The total momentum flux, being the integral in y of the total PV flux, is constant except in the immediate vicinity of the CLs, where it changes rapidly. The sign of $\gamma_j(y_{cj})$ determines whether the total momentum flux rises or falls at the CL in the jth layer. If it is positive, then the total momentum flux rises there with increasing y, while if it is negative, the total momentum flux falls there. And unlike in the barotropic case, there can be propagation (nonzero momentum flux) on both sides of a lower-layer CL. However, after an upper-layer CL (if there is one), under realistic conditions, the wave will be absorbed and the momentum flux will fall to zero. [Strictly speaking, the momentum flux falls to zero after an upper-layer critical latitude if and only if $|V_1^+ V_2^+| > (1/4)$, but for any realistic combinations of the parameters, that will be satisfied.]

If the flow is sufficiently slowly varying, then there will be negligible mixing of the two vertical modes, so that the amplitude ratio of the two layers will be well approximated by that of the external mode:

$$\frac{\psi_2(y)}{\psi_1(y)} = 2[\ell_{\text{ex}}^2(y) - V_1(y)]. \tag{32}$$

Departure from this amplitude ratio and the existence of an eddy heat flux is a sign of mode mixing, since the vertical phase tilt responsible for the heat flux is not present if the solution has the vertical structure of the external mode. Mode mixing is a distinctive feature of this two-layer scattering problem as compared to the single-mode barotropic problem.

It is also worth mentioning that on each side of the CL, one of the two squared meridional wavenumbers remains finite while the other blows up to $+\infty$ or $-\infty$ [neglecting the imaginary parts of $V_1(y)$ and $V_2(y)$]. Whether it is the external or internal mode that blows up on either side is determined by the sign of $V_2(y)$ as it approaches the CL. Whichever mode is finite on one side of the CL blows up on the other side. The implication of this is that one mode of the solution remains finite and bounded throughout the domain, but it switches between the external and internal modes as it crosses the CL.

We are interested in the ratio of the reflected total momentum flux at the southern limit to the incident total momentum flux, and in the ratio of the transmitted total momentum flux at the northern limit to the incident total momentum flux. Since the reflected momentum flux is positive and the incident and transmitted momentum fluxes are negative, the former is always negative and the latter is always positive. The absolute value of the former is the reflected flux and is denoted $\mathscr{R}$. The latter is the transmitted flux and is denoted $\mathscr{T}$.

At the northern limit, we only need to use the streamfunction to get the momentum flux of transmission. At the southern limit, we use the streamfunction and the boundary conditions to solve for the various coefficients of reflection, from which we can compute the incident momentum flux and the momentum flux due to reflection, and knowing those, we can calculate $\mathscr{R}$ and $\mathscr{T}$. When $\mathscr{R}$ is greater than 1, it is called overreflection, and when $\mathscr{T}$ is greater than 1, it is called overtransmission.

4. Baroclinic results

We begin with the baroclinic case with constant vertical shear, with a critical latitude in only the lower layer. Such a case is sketched in Fig. 4. We will examine one subcritical case and one supercritical case, which differ only in their vertical shear. The values of u^*, α, c, and k were chosen to match the values used in Fig. 2, after converting from our two-layer to our one-layer nondimensionalization. For each of these two baroclinic cases, we plot the amplitudes of the streamfunctions in both layers [$|\psi_1(y)|$ and $|\psi_2(y)|$], the amplitude ratio [$\psi_2(y)/\psi_1(y)$], and the momentum flux (in each layer and the total), all as a function of latitude y. We plot the

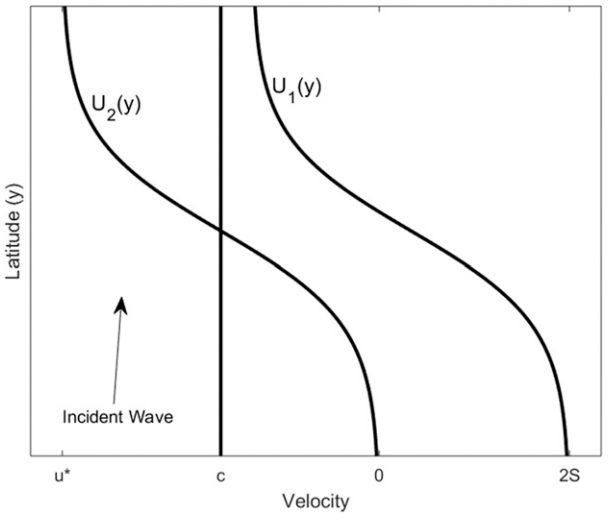

FIG. 4. Graph of the mean wind profiles for a baroclinic case with constant vertical shear $2S$ and with a critical latitude in only the lower layer.

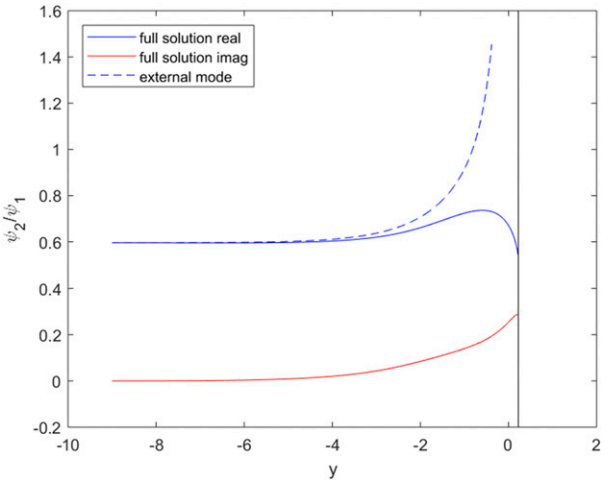

FIG. 6. The real and imaginary parts of the amplitude ratio $\psi_2(y)/\psi_1(y)$ and the external-mode amplitude ratio vs latitude for the subcritical case.

amplitude ratio only up to the critical latitude, and we plot the external-mode amplitude ratio for comparison. We also plot the heat flux on the same graph as the momentum fluxes. For the subcritical case, the streamfunction amplitudes are shown in Fig. 5, the amplitude ratios in Fig. 6, and the momentum and heat fluxes in Fig. 7. For the supercritical case, the streamfunction amplitudes are shown in Fig. 8, the amplitude ratios in Fig. 9, and the momentum and heat fluxes in Fig. 10.

We find that the reflected and transmitted flux (normalized by the incident flux), $(\mathscr{R}, \mathscr{T})$, is (0.0014, 0.552) in the subcritical case, and (0.0155, 2.84) in the supercritical case. As expected, there is a wave sink in the subcritical case and a source in the supercritical case. The transmission is totally dominant in both cases, for reasons that are not clear to us. In particular, the supercritical case exhibits overtransmission.

In both sub- and supercritical cases, both upper- and lower-level streamfunction amplitudes have a sinusoidal component toward the southern limit, with larger oscillations in the supercritical case. These oscillations are a sign of reflection and of interference between incident and reflected external waves. (The internal mode is evanescent near both the northern and southern boundaries.) Since $\mathscr{R}$ has a quadratic dependence on the reflected wave amplitude, noticeable oscillation can

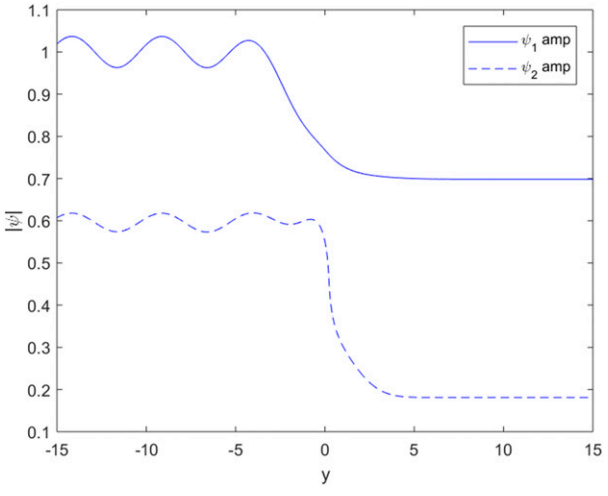

FIG. 5. Amplitudes of the streamfunctions in both layers, $|\psi_1(y)|$ and $|\psi_2(y)|$, vs latitude for the subcritical case. Here, $u^* = -0.9$, $\alpha = 0.5$, $c = -0.5$, $S = 0.85$, $k = 0.5$, $\varepsilon = 0.001$, and the gradient of mean PV at CL is 0.125. The result is $\mathscr{R} = 0.0014$ and $\mathscr{T} = 0.552$.

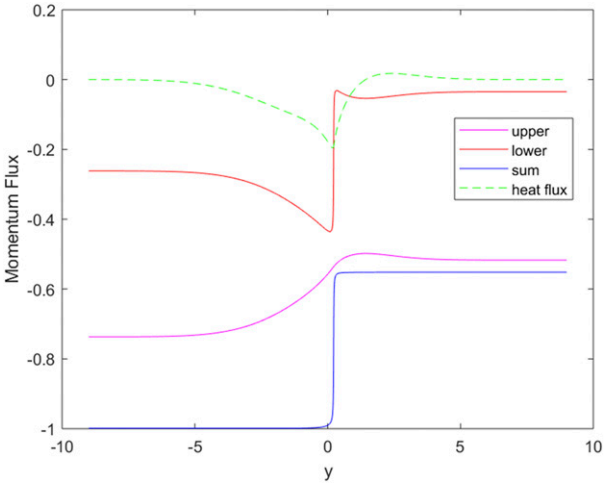

FIG. 7. Momentum flux in the upper layer, lower layer, and their sum, along with the heat flux, for the subcritical case.

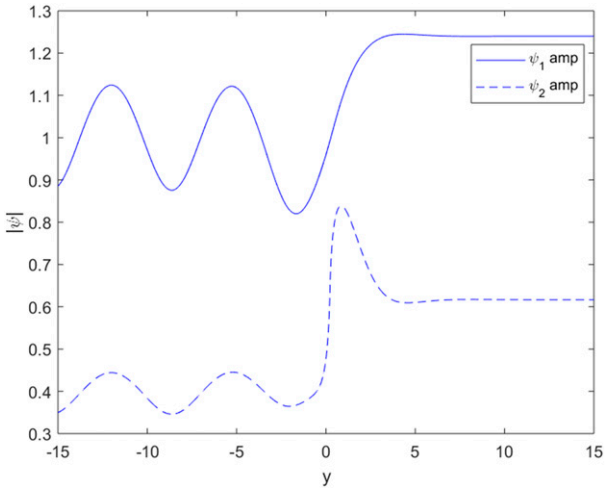

FIG. 8. Amplitudes of the streamfunctions in both layers, $|\psi_1(y)|$ and $|\psi_2(y)|$, vs latitude for the supercritical case. Here, $u^* = -0.9$, $\alpha = 0.5$, $c = -0.5$, $S = 1.15$, $k = 0.5$, $\varepsilon = 0.001$, and the gradient of mean PV at CL is -0.1747. The result is $\mathscr{R} = 0.0155$ and $\mathscr{T} = 2.84$.

exist even with $\mathscr{R}$ values as small as 0.0014 in the subcritical case. The constant value to the north of the shear zone indicates the constant amplitude of the transmitted external mode. We also see that for the subcritical case, the streamfunctions have a greater amplitude before the CL than after it, while for the supercritical case, the opposite is true, due to the overtransmission.

In the amplitude ratio graphs, we see that toward the southern limit, the amplitude ratio very closely matches the local external-mode structure, indicative of lack of mode-mixing, but this computed ratio deviates from the external-mode ratio as the CL is approached. At the CL,

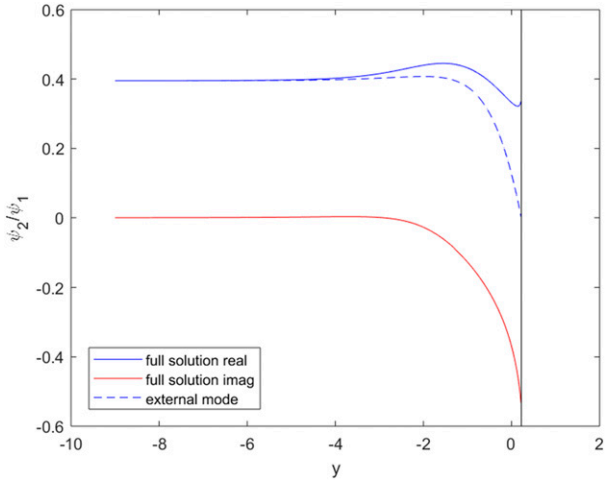

FIG. 9. The real and imaginary parts of the amplitude ratio $\psi_2(y)/\psi_1(y)$ and the external-mode amplitude ratio vs latitude for the supercritical case.

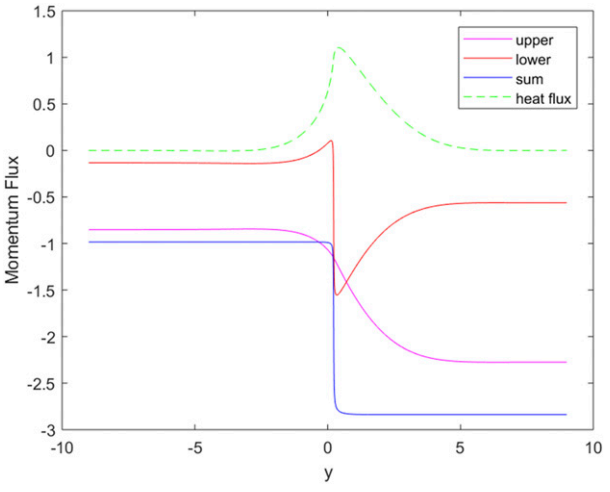

FIG. 10. Momentum flux in the upper layer, lower layer, and their sum, along with the heat flux, for the supercritical case.

the external-mode amplitude ratio (lower/upper) blows up to infinity in the subcritical case but approaches zero in the supercritical case. If there were no mode mixing, then one might imagine that in the supercritical case, the wave might propagate only through the upper layer, and critical layer behavior in the lower layer would be avoided by the vanishing streamfunction amplitude at the CL. But the figures clearly show that the actual amplitude ratio diverges from the external-mode ratio when we approach the CL, so this prediction is invalid, and singular behavior in the limit of vanishing damping does occur at the CL in both subcritical and supercritical cases.

In the momentum flux graphs, the quantity that behaves most simply, as expected, is the total momentum flux, which is constant throughout the domain except for the jump in the vicinity of the CL. The momentum flux increases with increasing y at the CL for the subcritical case and decreases at the CL for the supercritical case. We also see that in both cases, the lower-layer momentum flux changes rapidly at the CL while the upper-layer momentum flux changes gradually; this is because the heat flux is continuous at the CL, and using Eq. (30), this means that the jump in the lower-layer PV flux will cause a jump in the momentum flux only for the lower layer. The heat flux is negative throughout in the subcritical case but positive throughout in the supercritical case, with significant values in a fairly broad region around the CL, providing another indication for the region within which mode mixing occurs.

As discussed in Tung (1979), a Rossby wave in a region of positive PV gradient in a continuously stratified fluid will be refracted such that its ray path will approach a slanted critical line perpendicularly. In a configuration

in which the critical line slants equatorward with height, and starting with a horizontal ray path far from the CL, this implies downward propagation of wave activity and negative heat flux. We suspect that the negative heat flux in our subcritical case, in which the PV gradient is positive in both layers, is the two-layer analog to this continuous QG behavior. In a supercritical two-layer model, in contrast, we often think of the lower-layer PV gradient as analogous to the surface temperature gradient in the continuous theory, the reversal in sign of which is required for baroclinic instability if the interior (the upper layer in the two-layer model) has positive PV gradient. We do not claim to understand this fully. We suspect that the continuously stratified analog of the upward heat flux in our supercritical case would involve movement of wave activity from the surface reservoir to the interior reservoir, and not redistribution within the interior reservoir.

As the theory would predict, both the reflection and the transmission are considerably larger for the supercritical case than for the subcritical case. The supercritical case has overtransmission (although its reflection is still well below 1). For both cases, the transmission is much greater than the reflection. Again, the reasons for this are unclear, although calculations carried out by the authors but not reported in detail here indicate that as meridional shear is increased, the ratio of $\mathscr{R}$ to $\mathscr{T}$ typically increases.

Finally, we examine a very different case, in which S varies in latitude, and there is a critical latitude in both layers. This case is sketched in Fig. 11. We are using the vertical shear profile of

$$S(y) = \frac{1}{2}\Delta S[-\tanh(\alpha y) + 1] + S^{+}, \tag{33}$$

where S^{+} denotes the value of S at the northern limit, S^{-} the value at the southern limit, and ΔS the difference between S^{-} and S^{+}. We graph the streamfunction amplitude in both layers in Fig. 12 and the momentum and heat fluxes in Fig. 13.

This example is arguably more realistic than the previous two, thinking of decreasing S as approaching the tropics, although the potentially important increase in radius of deformation with decreasing latitude is still missing in this quasigeostrophic model. There are critical latitudes in both layers, as is the case in reality. The values of the parameters were chosen so that the shear is supercritical at the lower-layer CL. The PV gradient is positive at the upper-layer CL.

As expected, we find that $\mathscr{T}$ is virtually 0, as the wave cannot pass through the upper-layer CL, which completely absorbs the wave. This can be seen in both

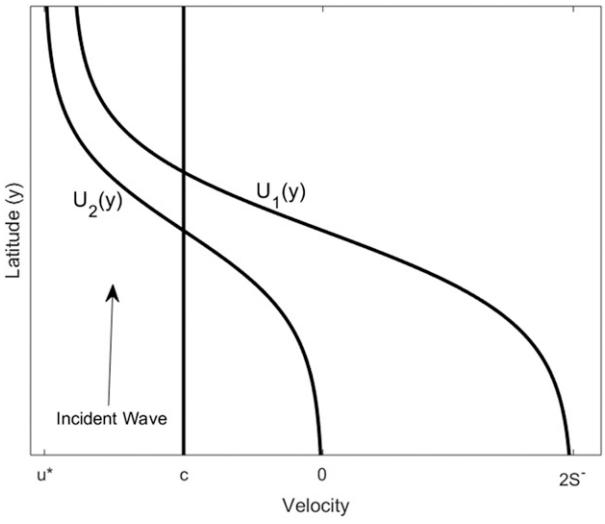

FIG. 11. Graph of the mean wind profile for a baroclinic case with a varying vertical shear $2S(y)$ and with critical latitudes in both layers.

Figs. 12 and 13: in Fig. 12, both streamfunctions vanish past the upper-layer CL, as do all the momentum and heat fluxes in Fig. 13. Qualitatively, as seen in Fig. 13, the lower-layer CL has the same effect on the momentum fluxes (and the heat flux) as it does in Fig. 10. Both the lower-layer momentum flux and the sum of the two momentum fluxes jump toward more negative values at the lower-layer CL, indicating overtransmission. There is also some reflection in this case, more so than in the cases examined above.

The overtransmission is modest in this case. The increase in amplitude of the total momentum flux across the lower-layer CL is roughly 20%. Therefore, the solution looks as if it is roughly passing through the lower-layer CL without being significantly modified. To this extent, the dominance of the upper-layer CL on the wave propagation evident in observations is captured.

We finish with a brief exploration of the conditions that favor smaller or larger amounts of transmission across the lower-layer critical latitude. Our results indicate that when the vertical shear toward the southern (incident) limit is increased, the reflection increases, while the transmission across the CL increases up to a point but then begins to decrease. Figure 14 illustrates this, as we plot the total momentum flux versus latitude for five profiles which differ only in their value of ΔS. The third of these profiles, which has $\Delta S = 1.2$, is the same profile as in Fig. 13. We see that only one of the five profiles, the one with the lowest value of ΔS, is subcritical at the lower-layer CL; the other four are all supercritical. And we see that as we increase ΔS, the

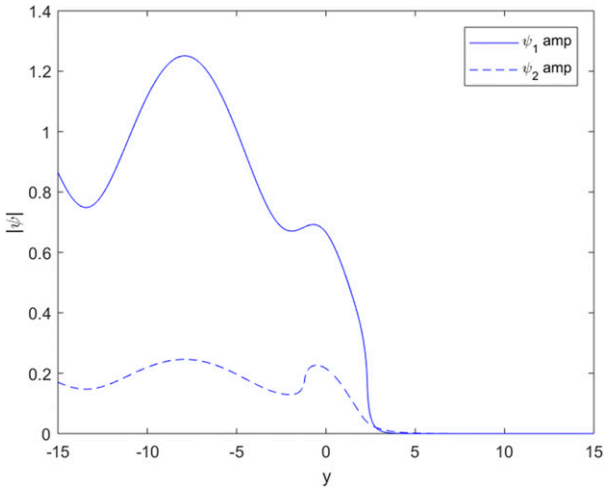

FIG. 12. Amplitudes of the streamfunctions in both layers, $|\psi_1(y)|$ and $|\psi_2(y)|$, vs latitude for the case with varying shear. Here, $u^* = -1.5$, $\alpha = 0.5$, $c = -0.35$, $\Delta S = 1.2$, $S^+ = 0.4$, $k = 0.5$, $\varepsilon = 0.001$, and the gradient of mean PV at lower-layer CL is -0.1769. The result is $\mathscr{R} = 0.0632$ and $\mathscr{T} \approx 0$.

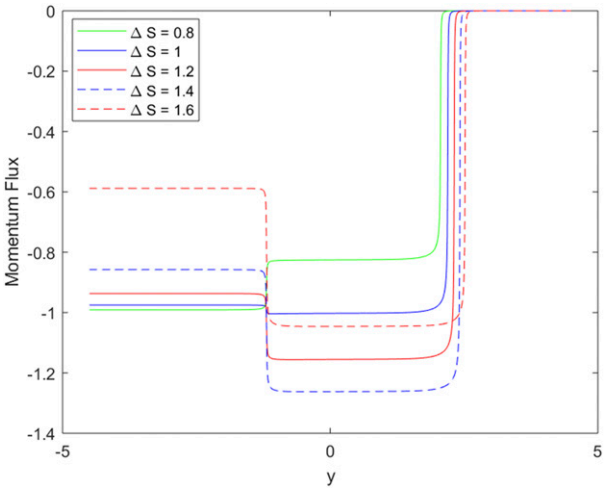

FIG. 14. Total momentum flux vs latitude for five different profiles, which differ only in their value of ΔS. All other parameters are as in Figs. 12 and 13.

reflection increases, while the transmission increases up until $\Delta S = 1.4$, after which it decreases sharply: the profile with the highest ΔS, $\Delta S = 1.6$, has the third-lowest transmission. Other results, which we do not include here, show that the transmission across the lower-layer CL tends to be higher when the phase speed is close to zero, and that other parameters, such as the meridional shear in the lower layer and the baseline vertical shear S^+, have little effect on the reflection or transmission. Even for this very idealized setting, the number of parameters is sufficient that it is difficult to describe the solutions throughout this parameter space,

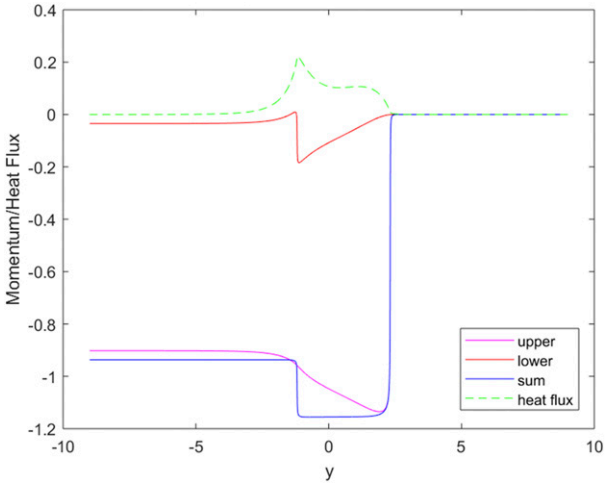

FIG. 13. Momentum flux in the upper layer, lower layer, and overall, along with the heat flux, for the case with varying shear.

and more theoretical guidance will be needed to isolate the parts of this space of most interest.

5. Conclusions

We have examined Rossby wave scattering problems in a quasigeostrophic two-layer model in the presence of critical latitudes (CLs), in which the singularity at these CLs is removed by a small amount of damping. The incoming wave in all cases was given the structure of the external mode of the two-layer system.

When the potential vorticity gradient is negative at the CL, theory indicates that the CL will act as a wave emitter. This emission can be realized as either overreflection, overtransmission, or a combination of the two. In all cases examined with a supercritical CL in the lower layer, we find overtransmission. In a case with a configuration most qualitatively similar to that found in the atmosphere, the wave first encounters a supercritical lower-tropospheric CL before encountering a subcritical CL in the upper troposphere. In this case, there is "temporary" overtransmission at the lower-layer CL before the wave is absorbed at the upper-level CL. If this overtransmission is of modest amplitude, then the solution gives the appearance of floating through the lower-layer CL without any CL-like dynamics occurring.

Overtransmission cannot occur in the barotropic case, since Rossby waves do not propagate on both sides of a CL. The two-layer setup described here may be the simplest system in which to study overtransmission through a single CL. Interaction between the two layers is essential. In particular, the upper-layer mean winds are essential for the propagation characteristics of the

external Rossby wave, an incident external mode being a natural way of setting up a useful scattering problem. We leave open the question of why overtransmission is ubiquitous in cases with a supercritical lower-layer CL and how the amplitude of the overtransmission is controlled.

In their study of the lower-tropospheric momentum fluxes in a statistically steady state of the quasigeostrophic two-layer model, Lutsko et al. (2017) describe the space-time spectra of the eddy momentum flux convergence, showing that this convergence is concentrated along the lower-layer CL for each phase speed in the wave field, especially for relatively long waves (see Fig. 4 of that paper). The scattering setup and the resulting overtransmission at the lower-layer CL described here may provide a plausible physical picture for interpreting the results in Lutsko et al. (2017). Following the familiar argument for the upper-layer CL, it may be possible to think of the wave–mean flow interaction at the lower-layer CL in terms of a wave excited near the center of the unstable jet and propagating outward. The wave cannot be thought of as a Rossby wave confined to the lower layer since such a disturbance would not propagate (this region is supercritical, so local Rossby wave propagation would require phase speeds greater than the mean westerly wind, precluding the existence of a lower-layer CL). Propagation by external-mode-like disturbances is possible out of the central supercritical region of the jet, however, as captured here in our simple scattering problem, and these could generate the mixing needed to create eddy fluxes of the sort described in Lutsko et al. (2017).

The two-layer vertical discretization seems at first glance to be an extremely crude representation of the atmosphere, so one could question the relevance of these results to the atmosphere on that basis alone. But Lutsko et al. (2017) show that a multilayer idealized GCM and a Southern Hemisphere reanalysis both show similar space–time spectra of the lower-tropospheric eddy momentum fluxes, providing indirect evidence for the qualitative relevance to the atmosphere of these scattering calculations.

Acknowledgments. Matthew Gliatto was supported by Award NA14OAR4320106 from the National Oceanic and Atmospheric Administration, U.S. Department of Commerce. The statements, findings, conclusions, and recommendations are those of the author(s) and do not necessarily reflect the views of the National Oceanic and Atmospheric Administration, or the U.S. Department of Commerce. We also wish to thank the reviewers, whose suggestions have led to the improvement of this paper.

REFERENCES

Charney, J. G., 1963: A note on large-scale motions in the tropics. *J. Atmos. Sci.*, **20**, 607–609, https://doi.org/10.1175/1520-0469(1963)020<0607:ANOLSM>2.0.CO;2.

Dickinson, R. E., 1968: Planetary Rossby waves propagating vertically through weak westerly wind wave guides. *J. Atmos. Sci.*, **25**, 984–1002, https://doi.org/10.1175/1520-0469(1968)025<0984:PRWPVT>2.0.CO;2.

——, 1969: Theory of planetary wave-zonal flow interaction. *J. Atmos. Sci.*, **26**, 73–81, https://doi.org/10.1175/1520-0469(1969)026<0073:TOPWZF>2.0.CO;2.

Geisler, J., and R. Dickinson, 1974: Numerical study of an interacting Rossby wave and barotropic zonal flow near a critical level. *J. Atmos. Sci.*, **31**, 946–955, https://doi.org/10.1175/1520-0469(1974)031<0946:NSOAIR>2.0.CO;2.

Halevy, I., and W. Peltier, 1985: Barotropic instability and Rossby wave radiation. *J. Atmos. Sci.*, **42**, 1825–1837, https://doi.org/10.1175/1520-0469(1985)042<1825:BIARWR>2.0.CO;2.

Held, I. M., 1983: Stationary and quasi-stationary eddies in the extratropical troposphere: Theory. *Large-Scale Dynamical Processes in the Atmosphere*, B. J. Hoskins and R. P. Pearce, Eds., Academic Press, 127–168.

Karoly, D. J., and B. J. Hoskins, 1982: Three dimensional propagation of planetary waves. *J. Meteor. Soc. Japan*, **60**, 109–123, https://doi.org/10.2151/JMSJ1965.60.1_109.

Killworth, P. D., and M. E. McIntyre, 1985: Do Rossby-wave critical layers absorb, reflect, or over-reflect? *J. Fluid Mech.*, **161**, 449–492, https://doi.org/10.1017/s0022112085003019.

Lindzen, R., and K. Tung, 1978: Wave overreflection and shear instability. *J. Atmos. Sci.*, **35**, 1626–1632, https://doi.org/10.1175/1520-0469(1978)035<1626:WOASI>2.0.CO;2.

——, B. Farrell, and K.-K. Tung, 1980: The concept of wave overreflection and its application to baroclinic instability. *J. Atmos. Sci.*, **37**, 44–63, https://doi.org/10.1175/1520-0469(1980)037<0044:TCOWOA>2.0.CO;2.

Lutsko, N. J., I. M. Held, P. Zurita-Gotor, and A. K. O'Rourke, 2017: Lower-tropospheric eddy momentum fluxes in idealized models and reanalysis data. *J. Atmos. Sci.*, **74**, 3787–3797, https://doi.org/10.1175/JAS-D-17-0099.1.

Phillips, N. A., 1956: The general circulation of the atmosphere: A numerical experiment. *Quart. J. Roy. Meteor. Soc.*, **82**, 123–164, https://doi.org/10.1002/qj.49708235202.

Potter, S. F., T. Spengler, and I. M. Held, 2013: Reflection of barotropic Rossby waves in sheared flow and validity of the WKB approximation. *J. Atmos. Sci.*, **70**, 2170–2178, https://doi.org/10.1175/JAS-D-12-0315.1.

Randel, W. J., and I. M. Held, 1991: Phase speed spectra of transient eddy fluxes and critical layer absorption. *J. Atmos. Sci.*, **48**, 688–697, https://doi.org/10.1175/1520-0469(1991)048<0688:PSSOTE>2.0.CO;2.

Tung, K., 1979: A theory of stationary long waves. Part III: Quasi-normal modes in a singular waveguide. *Mon. Wea. Rev.*, **107**, 751–774, https://doi.org/10.1175/1520-0493(1979)107<0751:ATOSLW>2.0.CO;2.

Webster, P. J., and J. R. Holton, 1982: Cross-equatorial response to middle-latitude forcing in a zonally varying basic state. *J. Atmos. Sci.*, **39**, 722–733, https://doi.org/10.1175/1520-0469(1982)039<0722:CERTML>2.0.CO;2.

Yamada, M., and M. Okamura, 1984: Overreflection and overtransmission of Rossby waves. *J. Atmos. Sci.*, **41**, 2531–2535, https://doi.org/10.1175/1520-0469(1984)041<2531:OAOORW>2.0.CO;2.